Planta
https://doi.org/10.1007/s00425-018-2883-0

ORIGINAL ARTICLE

Ectopic expression of *VpSTS29*, a stilbene synthase gene from *Vitis pseudoreticulata*, indicates STS presence in cytosolic oil bodies

Fuli Ma[1,2,3] · **Lei Wang**[1,2,3] · **Yuejin Wang**[1,2,3]

Received: 22 November 2017 / Accepted: 17 March 2018
© Springer-Verlag GmbH Germany, part of Springer Nature 2018

Abstract

Main conclusion **Stilbene synthase (STS) and its metabolic products are accumulated in senescing grapevine leaves. Ectopic expression of *VpSTS29* in *Arabidopsis* shows the presence of VpSTS29 in oil bodies and increases *trans*-piceid in developing leaves.**

Stilbenes are the natural antimicrobial phytoalexins that are synthesised via the phenylpropanoid pathway. STS is the key enzyme catalysing the production of stilbenes. We have previously reported that the *VpSTS29* gene plays an important role in powdery mildew resistance in *Vitis pseudoreticulata*. However, the synthesis and accumulation of these stilbene products in plant cells remain unclear. Here, we demonstrate that VpSTS29 is present in cytosolic oil bodies and can be transported into the vacuole at particular plant-developmental stages. Western blot and high-performance liquid chromatography showed that STS and *trans*-piceid accumulated in senescent grape leaves and in *pVpSTS29*::*VpSTS29*-expressing *Arabidopsis* during age-dependent leaf senescence. Subcellular localisation analyses indicated VpSTS29-GFP was present in the cytoplasm and in STS-containing bodies in *Arabidopsis*. Nile red staining, co-localisation and immunohistochemistry analyses of leaves confirmed that the STS-containing bodies were oil bodies and that these moved randomly in the cytoplasm and vacuole. Detection of protein profiles revealed that no free GFP was detected in the *pVpSTS29*::*VpSTS29*-GFP-expressing protoplasts or in *Arabidopsis* during the dark–light cycle, demonstrating that GFP fluorescence distributed in the STS-containing bodies and vacuole was the VpSTS29-GFP fusion protein. Intriguingly, in comparison to the controls, over-expression of *VpSTS29* in *Arabidopsis* resulted in relatively high levels of *trans*-piceid, chlorophyll content and of photochemical efficiency accompanied by delayed leaf senescence. These results provide exciting new insights into the subcellular localisation of STS in plant cells and information about stilbene synthesis and storage.

Keywords Chinese wild grape · Stilbene synthase gene · Expression profile · Subcellular localisation · Oil body · Leaf senescence

Abbreviations

GFP	Green fluorescent protein
HPLC	High-performance liquid chromatography
STS	Stilbene synthase
CLO3	Caleosin 3

Introduction

Unlike many autotrophic marine organisms, land plants are unable to move. Hence, they must instead mitigate any stressful situation in which they find themselves, repair any damage done and perhaps adjust to that situation in such a way as to minimise future damages (Roy 2000). In consequence, plants produce many thousands of secondary

Electronic supplementary material The online version of this article (https://doi.org/10.1007/s00425-018-2883-0) contains supplementary material, which is available to authorized users.

✉ Yuejin Wang
wangyj@nwsuaf.edu.cn

[1] College of Horticulture, Northwest A & F University, No. 3 Taicheng Road, Yangling 712100, Shaanxi, People's Republic of China

[2] Key Laboratory of Horticultural Plant Biology and Germplasm Innovation in Northwest China, Ministry of Agriculture, Yangling 712100, Shaanxi, People's Republic of China

[3] State Key Laboratory of Crop Stress Biology in Arid Areas, Northwest A&F University, Yangling 712100, Shaanxi, People's Republic of China

Published online: 27 March 2018

metabolites to strengthen their defences against various stresses (Dixon 2001). Stilbene phytoalexins are secondary metabolites that are rapidly accumulated in response to biotic and abiotic stresses, such as pathogen infection and UV irradiation (Dercks and Creasy 1989; Hammerbacher et al. 2011; Suzuki et al. 2015; Hain et al. 1993). Resveratrol and its derivatives, which are synthesised via the phenylpropanoid pathway, were first extracted and identified from the *Vitaceae* by Langcake and Pryce (1976). However, little information is available on their synthesis and potential functions in plant growth and development.

L-Phenylalanine, the entry point from the shikimate pathway to the phenylpropanoid pathway, was previously reported to be synthesised in chloroplasts (Jung and Jensen 1986; Rippert et al. 2009). Studies on subcellular localizations have also documented that the downstream products in this metabolic channelling seem to shift from the chloroplasts to the endoplasmic reticulum (ER) (Jørgensen et al. 2005). Phenylalanine ammonia lyase isoform 1 (*PAL1*) is localised to the ER but another isoform *PAL2* is recruited from the cytosol to the ER when co-localised with the ER-localised cinnamate 4-hydroxylase (*C4H*) in transgenic tobacco (Ro et al. 2001; Achnine et al. 2004). Next, 4-coumarate: CoA ligases (*4CLs*), catalyse the third step of the phenylpropanoid pathway, showing distinct roles in the downstream branch pathways; especially *4CL1* which is localised near to the ER and contributes to the total enzymatic activity (Bassard and Werck-Reichhart 2012). These previous findings support the model that ER-associated multi-enzyme complexes comprising the first three enzymes of the phenylpropanoid pathway, coordinate the metabolic channelling (Winkel 2004) and different metabolons are organised by different 4-coumarate: CoA Ligase isoforms (Ehlting et al. 1999; Li et al. 2015).

The forth step is catalysed either by stilbene synthase (STS) or chalcone synthase (CHS), which are two related polyketide synthases using one p-coumaroyl-CoA and three malonyl-CoA as substrates (Ferrer et al. 1999; Fritz and Klaus 1975; Tropf et al. 1994). STSs, the key enzymes catalysing the production of the stilbene backbone, belong to a multigene family, which was previously reported to possess 48 members in *Vitis vinifera* (Parage et al. 2012; Vannozzi et al. 2012). At least nine *STS* members have been experimentally identified with functional enzymatic activities (Parage et al. 2012). Although these functional members were reported, the dynamic subcellular distributions of the STSs in response to environmental stimulus are still unclear.

Immune-histochemical and immunogold electron-microscope techniques have been used to determine the distribution of STSs in vivo (Fornara et al. 2008). The STS signal was found to be present in the five selected organs of *V. vinifera* cv. Cabernet Sauvignon, and immunogold particles labelled in the cytoplasm and cell walls with special cases that some particles are also located in the vacuoles of the roots, the chloroplasts of the stem and the nuclei and chloroplasts of the leaf (Wang et al. 2010). The STS protein is also present throughout the development of the grape berry (Pan et al. 2009) and predominantly enriched in the exocarp (Fornara et al. 2008). Further studies demonstrated that STS resides mainly in the cell wall and cytoplasm of the fruit skin (Fornara et al. 2008; Pan et al. 2009). These multiple subcellular locations of STS prompt us to explore the flow of STS after their formation to their final destinations.

China is one of the centres of origin of *Vitis* plants with plentiful wild germplasm resources (Wang et al. 1995). Observation from several decades of field trails demonstrated *V. pseudoreticulata* accession Baihe-35-1 is a germplasm with a high degree of resistance to powdery mildew (caused by the fungus *Erysiphe necator*). Several disease resistance-related genes, including *STS* genes, have been isolated and functionally validated, demonstrating that these respond functionally to *E. necator*, salicylic acid, methyl jasmonate, wounding and UV-C radiation (Jiao et al. 2016; Yin et al. 2016; Xu et al. 2011). In particular, a STS gene *VpSTS29* (GenBank Accession: MF498770) from *V. pseudoreticulata* with a sequence variation (Ser-to-Phe) in the conserved motif IPNSAGAIAGN had been shown to accumulate stilbene compounds in response to stresses (Xu et al. 2010, 2011). In this study, we investigated the expression profiles and subcellular distributions of *VpSTS29* both in grapevines and in transgenic *Arabidopsis* plants during age-dependent and dark-induced senescence. Monitored by green fluorescence protein, *VpSTS29* was co-localised with organelle marker gene fused at the C-terminal of mCherry by the *Arabidopsis* mesophyll protoplast transient gene expression system. A time course confocal microscopy observation was carried out to record the behaviour of VpSTS29 after its location into STS-containing bodies. The final destination of VpSTS29 was analysed by transmission electron microscopy and immunohistochemistry during dark-promoted senescence. We also investigated the delay of leaf senescence in transgenic *Arabidopsis* over-expressing *VpSTS29*. The study provides useful insight into the localisation of STS into oil bodies and the potential destination for stilbene storage.

Materials and methods

Plant materials and growth conditions

One-year-old *V. Vinifera* cv. Thompson Seedless were transplanted to an environmental growth chamber and cultured until each plant had 15 fully expanded leaves. For the dark treatment, the plantlets were incubated for 8 days under dark conditions starting from the end of an 8 h dark cycle. The control was kept for 8 days at 25 °C under a 16/8 h light/

dark photoperiod with illumination of 100 µmol m^{-2} s^{-1}. T3 transgenic *Arabidopsis* (CaMV35S-GFP, *VpSTS29*-OE and p*VpSTS29*::*VpSTS29*-GFP) and Columbia ecotype Col-0 seeds were placed on wet filter paper and vernalised for 3 days at 4 °C in the dark. After incubation in the light for 2 days at 22 °C, seedlings were transferred to a soil mix at 22 °C under a 16/8 h light/dark photoperiod.

Expression of *STS29* in developing and senescing leaves and generation of *VpSTS29*-OE and p*VpSTS29*::*VpSTS29*-GFP transgenic *Arabidopsis*

Expression profiles of *MYB13, MYB14, MYB15* and *STS29* in developing and senescing grapevine leaves were analysed according to the datasets of Gene Expression Omnibus (no. GSE36128). The primers *STS29*-F/R (Höll et al. 2013) were used to quantify the total expression levels of *STS25*, *STS27*, and *STS29* in different leaf positions and after darkness had been initiated. *VvGAPDH* (GenBank accession No. EF192466) was used as a control. Quantitative real-time PCR was carried out on three replicates using a SYBR Green method and an IQ5 real-time PCR detection system (Bio-Rad).

The 1179 bp *Kpn* I-*Bam* H I full-length *VpSTS29* was amplified with cDNAs from *V. pseudoreticulata* Baihe 35-1 using the forward primer (5′-AGAACACGGGGGACGAGC TCATGGCTTCAGTTGAGGAAATTAGAAACGATC-3′) and reverse primer (5′-ACCATGGTGTCGACTCTAGAA TTTGTAACCATAGGAATGCTATGCAACA-3′) and then inserted into the same restriction sites of vector pCAMBIA2300-CaMV35S-GFP to generate *VpSTS29*-GFP. The CaMV35S of the vector *VpSTS29*-GFP was replaced by the 1172 bp promoter region of *VpSTS29* (Xu et al. 2011) to generate p*VpSTS29*::*VpSTS29*-GFP. The vectors carrying *VpSTS29*-GFP and p*VpSTS29*::*VpSTS29*-GFP were introduced into *Rhizobium radiobacter* strain GV3101 and then transformed into wild-type *Arabidopsis* Col-0 using the floral dip method (Clough and Bent 1998) to generate *VpSTS29-OE* and p*VpSTS29*::*VpSTS29*-GFP transgenic *Arabidopsis*, respectively. The transgenic *Arabidopsis* lines were identified by western blot using GFP antibodies and grape STS antibodies, respectively. Three independent T3 transgenic plants were used for function analysis.

To construct the 35S-mCherry translational fusion protein, the coding sequence of *mCherry* was amplified from pmCherry-N1 vector (Clontech, USA) using the forward primer (5′-GCTCTAGAGTCGCCACCATGGTGAGCAA-3′) and reverse primer (5′-GGAGCTCAGATCTGGATC CCCCGGGCTTGTACAGCTCGTCCATGCC-3′). The coding sequence of mCherry was inserted into the vector pCAMBIA2300-35S-GFP between the *Sal* I and *Pst* I restriction sites to replace the GFP to generate pCAMBIA2300-35S-mCherry (35S-mCherry). The open-reading frame of the oil body marker CLO3 (Shimada et al. 2014) was amplified from *A. thaliana* using the forward primer (5′-ACGAGCTGTACAAGCCCGGGATGGCAGGAGAGG CAGAGG-3′) and the reverse primer (5′-GATCGGGGA AATTCGAGCTCTTAGTCTTGTTTGCGAGAATTGGCC-3′) and cloned into the C-terminal of 35S-mcherry between the *Sma* I and *Sac* I restriction sites to generate mCherry-CLO3. All the constructs were sequenced.

Determination of stilbenes by high-performance liquid chromatography

Leaves from the age-dependent- and dark-induced senescent leaves of grapevine and transgenic *Arabidopsis* were dried in a vacuum freeze drying chamber for 48 h in the dark and extracted in methanol for another 24 h at 4 °C. The content of *trans*-resveratrol, *cis*-piceid and *trans*-piceid were determined according to the method of Cheng et al. (2016).

Arabidopsis protoplast-transient assay and cell imaging with laser scanning confocal microscopy

Isolation of protoplasts from the young or senescent leaves of the p*VpSTS29*::*VpSTS29*-GFP transgenic *Arabidopsis* was carried out according to the protocol of Yoo et al. (2007). Prior to the isolation, aerial parts of the 4-week-old transgenic *Arabidopsis* plants were transferred to darkness for 7 days to induce leaf senescence (Shimada et al. 2014). For the GFP/mcherry co-localisation experiments, 20 µg of plasmid DNA of mCherry-tagged oil body marker CLO3 genes was transiently co-expressed in protoplasts isolated from the young or senescent leaves of the transgenic *A. thaliana* using PEG transformation assays. The protoplasts were then cultured either at room temperature under normal light conditions for 24 h or in darkness for 24 h. Cell imaging with laser scanning confocal microscopy (LSCM) was carried out with the Olympus FluoView™ FV1000 system. For the time-lapse experiment, the co-localisation of VpSTS29-GFP was imaged every 7 s to monitor the movement of VpSTS29-GFP-labeled bodies in the cytoplasm.

For the GFP/Nile red co-localisation experiments, protoplasts were stained with Nile red (MP Biomedicals, USA) according to the manufacturer's instructions. For GFP/Nile red/mCherry labelling (Thazar-Poulot et al. 2015), protoplasts were sequentially excited at 488 and 561 nm, and emissions were recovered between 500 and 530 nm (GFP), between 560 and 590 nm (Nile red) and between 595 and 630 nm (mCherry). Chloroplast autofluorescence was excited at 630 nm and collected from 670 to 730 nm. Quantitative analysis of the co-localisation of oil bodies stained with Nile red and labelled with VpSTS29-GFP was counted from five fluorescence images. A total of 80 oil bodies were examined. Quantitative analysis of the co-localisation of

VpSTS29-GFP and mCherry-CLO3 were carried out in protoplasts isolated from young and senescent leaves. A total of 33 oil bodies in four confocal images from young leaves and a total of 95 oil bodies in five confocal images from senescent leaves were counted.

Transmission electron microscopy (TEM) analysis

To observe the ultrastructure change induced by darkness for 4 days, the leaves of grapevine were collected and cut into 1 × 2 mm rectangles to prepare for ultrathin sectioning. TEM analysis was carried out as previously described by Xu et al. (2014).

Western blot and immunohistochemistry (IHC) analysis

Protein extraction and concentration measurement were carried out according to the method described by Kambiranda et al. (2014). Grape STS antibodies were obtained according to the conserved N terminus (aa 1–184) (Shanghai ImmunoGen Biological Technology Co., Ltd). Samples (30 μg) of total protein were subjected to denaturing SDS-PAGE and immunoblot analysis carried out using antibodies against grape STS, GFP (TransGen Biotech, China) and mCherry (Abbkine, USA). Goat anti-Rabbit IgG (H+L) (TransGen Biotech, China) was obtained to recognise the rabbit polyclonal anti-STS antibodies and goat anti-mouse IgG (H+L) (TransGen Biotech, China) was obtained to recognise the mouse monoclonal anti-GFP and anti-mCherry antibodies. All the primary antibodies were diluted 1:1000 and secondary antibodies diluted 1:5000.

Immunocytolocalisation of STS using antibodies against grape STS in sections of grapevine leaves were carried out as previously described (Gomez et al. 2011). The primary antibodies were diluted 1:200 and the secondary antibodies (anti-rabbit IgG conjugated to the Alexa Fluor 488 fluorochrome) were diluted 1:500.

The analysis of VpSTS29-GFP protein profile

For the determination of VpSTS29-GFP protein profile when co-expressed with mCherry-*CLO3*, different contents of plasmid mCherry-*CLO3* were transiently expressed in the protoplasts isolated from the p*VpSTS29*::*VpSTS29*-GFP transgenic plants. For the determination of VpSTS29-GFP protein profile during dark-induced senescence, the 2-week-old p*VpSTS29*::*VpSTS29*-GFP transgenic plants were transferred to dark conditions (D) for 12, 24, 48 or 72 h and then incubated under light conditions (*L*) for 1, 2, 4, 6 or 12 h. The samples were collected at the times indicated and total protein (20 μg) was subjected to immunoblotting with anti-mCherry and anti-GFP antibodies, respectively.

Measurements of chlorophyll contents and photochemical efficiency of PSII

For age-dependent leaf senescence, the fourth rosette leaf of individual *VpSTS29*-OE transgenic plants was collected 3, 4, 5 or 6 weeks after sowing and used for analyses of stilbene content (Cheng et al. 2016), chlorophyll content (Li et al. 2013) and photochemical efficiency of PSII (Oh et al. 1997). The results were calculated from six leaves in each experiment and are shown as the relative percentage to the first point value for each experiment.

Statistical analysis

The means and standard deviation (SD) were obtained from three independent experiments. SPSS 22.0 software was used for statistical analysis. The significant difference analysis was assessed by the least significant difference (LSD) test ($*P < 0.05$; $**P < 0.01$).

Results

Stilbene synthase is partially expressed in age-dependent and dark-induced senescent leaves of grapevine

The R2R3-MYB transcription factors, MYB13, MYB14 and MYB15, have been reported to regulate the biosynthesis of stilbenes (Höll et al. 2013; Dubrovina and Kiselev 2017). Thus, the expression profiles of these transcription factors were analysed according to the datasets of Gene Expression Omnibus (no. GSE36128). As expected, *VvMYB13* and *VvMYB15* but not *VvMYB14* were induced in senescing leaves (Supplemental Fig. S1a).

To gain insight into the expression of STS and the accumulation of stilbenes in senescing leaves, detection of a vertical gradient from near the base (defined as the 1st leaf) to the apex (defined as the 12th leaf) was analysed in 1-year-old *V. Vinifera* cv. Thompson Seedless plantlets (Fig. 1a). Western blot analysis using the anti-STS antibodies indicates that STS was present in all leaves from the base to the apex but especially accumulated in the mature to senescent basal leaves. Of interest were observations that a minimum content of *trans*-resveratrol and a significant accumulation of *trans*-piceid (the glycosylated resveratrol derivative) in senescent leaves were determined by HPLC (Fig. 1b).

It has been reported that dark treatment can be used to induce senescence in plants (Weaver and Amasino 2001). We, therefore, tested for STS expression following 8 days of darkness. The shoot tips were cut off to promote the germination of buds during the dark treatment. Compared with the controls, cultured under normal light/dark conditions,

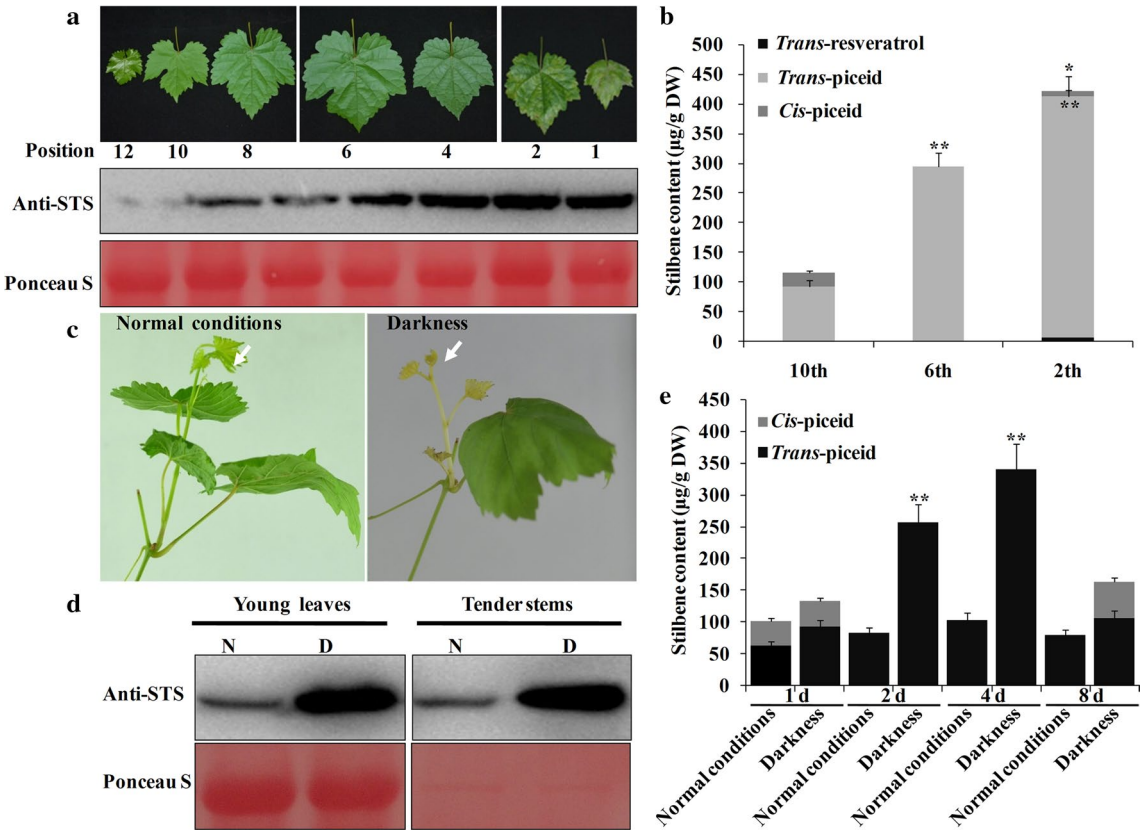

Fig. 1 Stilbene synthase is accumulated in senescent leaves of grapevine. **a** The levels of stilbene synthase protein from different positions on 1-year-old of *Vitis vinifera* var. Thompson Seedless plants with 15 leaves. Counting from near the base, the leaves are referred to as the 1st to the 12th (apex). Extracts from leaves were subjected to western blot with a specific antibody against grape STS. **b** HPLC analysis of stilbene compounds in the representative development stages of leaves. The significant difference test was assessed by the least significant difference (LSD) test (**$P < 0.01$). Error bars show standard deviation from three independent experiments. **c** The phenotypes during artificially induced senescence. The shoot tips were cut off before the dark treatment. The control was cultured under normal conditions with 16 h light/8 h dark at 25 °C. The dark treatment was continuous for eight days at 25 °C. **d** The change in stilbene synthase protein in leaves and stems after the dark treatment. Leaves and stems were collected for western blot analysis using grape STS antibodies. **e** HPLC analysis of stilbene compounds in leaves incubated under dark conditions. Samples were collected at 1, 2, 4 and 8 days after dark treatment. Leaves incubated under normal conditions were used as the control. The significant difference test was assessed by the least significant difference (LSD) test (**$P < 0.01$). Error bars show SD from three independent experiments

the young leaves of dark/dark plants showed weaker growth and chlorosis (Fig. 1c). In addition, the amounts of STS protein in both the young leaves and stems were significantly elevated after the dark treatment (Fig. 1d). Meanwhile, the content of *trans*-piceid was significantly increased after 2–4 days' treatment but was decreased to the same level as under normal conditions at 8 days (Fig. 1e). These results show senescence enhances the expression of STS in young tissues.

Ectopic expression of *VpSTS29* in *Arabidopsis thaliana* increases the accumulation of STS and stilbene content in senescent leaves

STS29 is induced by biotic or abiotic stress and strongly regulated by *MYB15* (Höll et al. 2013). It is also expressed in senescent leaves and dark-induced leaves on day 4 (Supplemental Fig. S1b–d). Therefore, *STS29* was selected as the representative member to explore the function of STS during leaf senescence. To determine the ubiquitous response of STS in different *Vitis* species, *VpSTS29* (homologous to *VvSTS29*) from *V. pseudoreticulata* accession Baihe-35-1 (Xu et al. 2011) was isolated, fused with green fluorescent protein (GFP) in its C-terminal region and then ectopically expressed in *A. thaliana* under the control of its native promoter. CaMV35S-GFP was used as the positive control. Western blot analysis showed the GFP fusion protein was expressed in the T3 transgenic *Arabidopsis* plants (Fig. 2a). The 2- and 5-week-old CaMV35S-GFP and p*VpSTS29*::*VpSTS29*-GFP-expressing plants were used to monitor the expression of STS and the accumulation of stilbenes during age-dependent

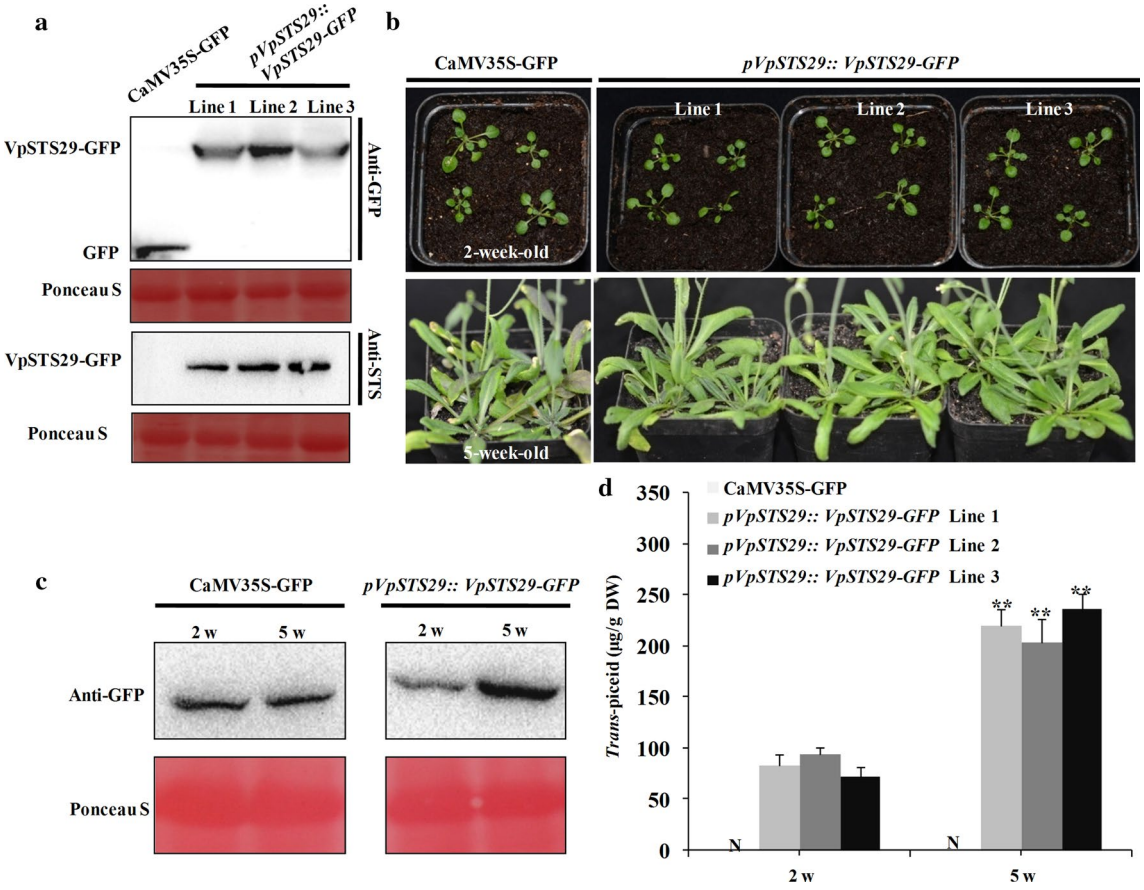

Fig. 2 Expression of *VpSTS29* from *Vitis pseudoreticulata* accession Baihe-35-1 leads to the increase of *trans*-piceid in *Arabidopsis*. **a** The identification of p*VpSTS29*::*VpSTS29-GFP* expressing transgenic *Arabidopsis*. Extracts (20 μg) from *Arabidopsis* leaves were subjected to western blot with specific antibodies against green fluorescing protein (GFP) and grape STS, respectively. CaMV35S-GFP-expressing transgenic *Arabidopsis* was used as the positive control. **b** The phenotype images of 2- and 5-week-old p*VpSTS29*::*VpSTS29-GFP* expressing transgenic plants. **c** The expression of VpSTS29 protein in leaves of transgenic plants. Extracts from leaves of 2- and 5-week-old transgenic plants were subjected to western blot with a specific antibody against GFP. Three biological replicates were carried out with similar results. **d** HPLC analysis of stilbene compounds in 2- and 5-week-old transgenic plants. N indicates that no stilbene compound was detected. The significant difference test was assessed by the least significant difference (LSD) test ($*P < 0.05$). Error bars show SD from three independent experiments

leaf senescence (Fig. 2b). Immunoblotting detection of VpSTS29-GFP fusion protein using anti-GFP antibodies showed that VpSTS29 was induced in senescent leaves of the transgenic plants (Fig. 2c). To investigate the activity of VpSTS29 protein in the transgenic plants, HPLC was also carried out to determine the stilbene content in the 2- and 5-week-old leaves. No stilbenes were detected in leaves of the positive control (Fig. 2d). Conversely, *trans*-piceid, which has previously been determined to be the form of stilbenes in transgenic *Arabidopsis* (Huang et al. 2016; Jiao et al. 2016), was identified in both 2- and 5-week-old transgenic plants and the total content in the 5-week-old plants was approximately three times higher than that in the 2-week-old plants. Together, these results indicate the representative *STS29* gene can encode protein-exhibiting STS activity when ectopically expressed in *A. thaliana*, thus resulting in increased *trans*-piceid content in developing leaves.

VpSTS29 is located in the cytoplasm and translocated into STS-containing bodies under dark-induced senescence

In the light of the findings that STS and its metabolic products are accumulated in senescent leaves, it was considered worthwhile to investigate how senescence might promote the activity of functional STS enzymes. We first detected differences in the subcellular distribution of VpSTS29 in young and senescent leaves. Prior to isolating the protoplasts, the aerial parts of both CaMV35S-GFP and p*VpSTS29*::*VpSTS29*-GFP transgenic plants were transferred to the dark for 7 days to generate senescent leaves.

When driven by its native promoter, the fluorescence signal of VpSTS29-GFP in the transgenic *Arabidopsis* protoplasts isolated from leaves grown under normal conditions was distributed in the cytoplasm between the chloroplasts (Fig. 3a). In protoplasts isolated from senescent leaves, VpSTS29-GFP was also located in some spherical structures (Fig. 3b). The GFP fluorescence signal of the positive control was not changed in the protoplasts under normal conditions nor in the dark treatment (Fig. 3c).

The VpSTS29-containing bodies observed above may indicate the result of redistribution of STS protein in response to dark-induced senescence. Time-lapse imaging was used to record the behaviours of the STS-containing bodies in the cytoplasm. Our results from *Arabidopsis* protoplasts isolated from leaves grown under dark treatment demonstrated that the VpSTS29-containing bodies were initially close to GFP-tagged VpSTS29 and later exhibited Brownian movement in the cytoplasm (Fig. 4, bodies marked by white arrows). Together, our results show that VpSTS29 is located in the cytoplasm under normal conditions and translocated into STS-containing bodies under dark-induced senescence.

VpSTS29-containing bodies are leaf oil bodies

Due to the presence of VpSTS29-GFP in the cytoplasm and also in some spherical bodies, inter-organelle communication of VpSTS29-GFP may have occurred in senescent leaves. To monitor protein transport, we determined the nature of the STS-containing bodies. As has been reported, ER can direct the biogenesis of certain membrane organelles such as ER bodies and autophagosomes (Bernales et al. 2006; Herman 2008). Hence, we hypothesised that the STS-containing bodies might be related to oil bodies which function as subcellular sites for the synthesis of phytoalexin in *Arabidopsis* (Shimada et al. 2014). To this end, leaf protoplasts isolated from young leaves were stained with Nile red, a dye specially targeting lipid droplets/oil bodies (Greenspan et al. 1985). As expected, VpSTS29-GFP was partially localised to the Nile red-stained oil bodies (Fig. 5a,

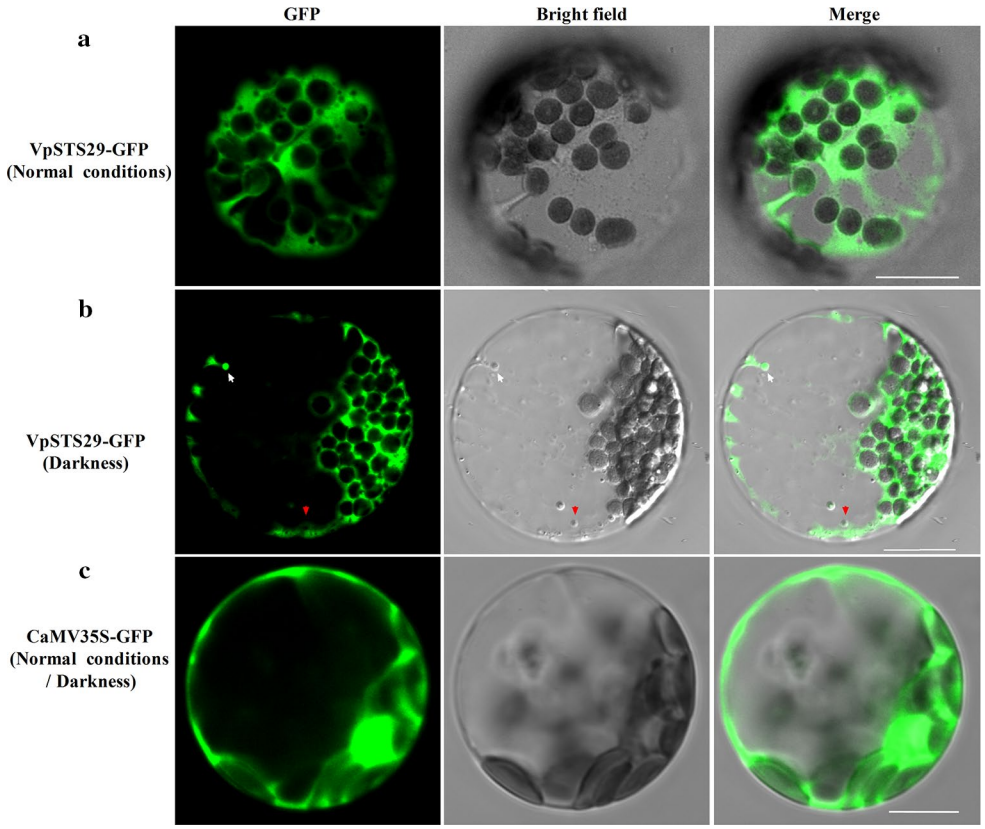

Fig. 3 Subcellular distribution of VpSTS29 in p*VpSTS29*::*VpSTS29-GFP* expressing transgenic *Arabidopsis*. **a** Subcellular location of VpSTS29 in leaves incubated under normal conditions. Protoplasts were separated from the young leaves of p*VpSTS29*::*VpSTS29-GFP* expressing transgenic *Arabidopsis* and observed by confocal laser scanning microscopy. Scale bar = 10 μm. **b** Subcellular location of VpSTS29 in leaves incubated in darkness. The aerial parts of p*VpSTS29*:: *VpSTS29*-GFP transgenic plants were transferred to dark conditions for 7 days to generate senescent leaves. Protoplasts were separated and observed by confocal laser scanning microscopy. The white arrow indicates the STS29-positive bodies. The red arrow indicates the STS29-negative bodies. Scale bar = 10 μm. **c** Subcellular distribution of CaMV35S-GFP in leaves incubated under normal conditions or in darkness. Scale bar = 10 μm

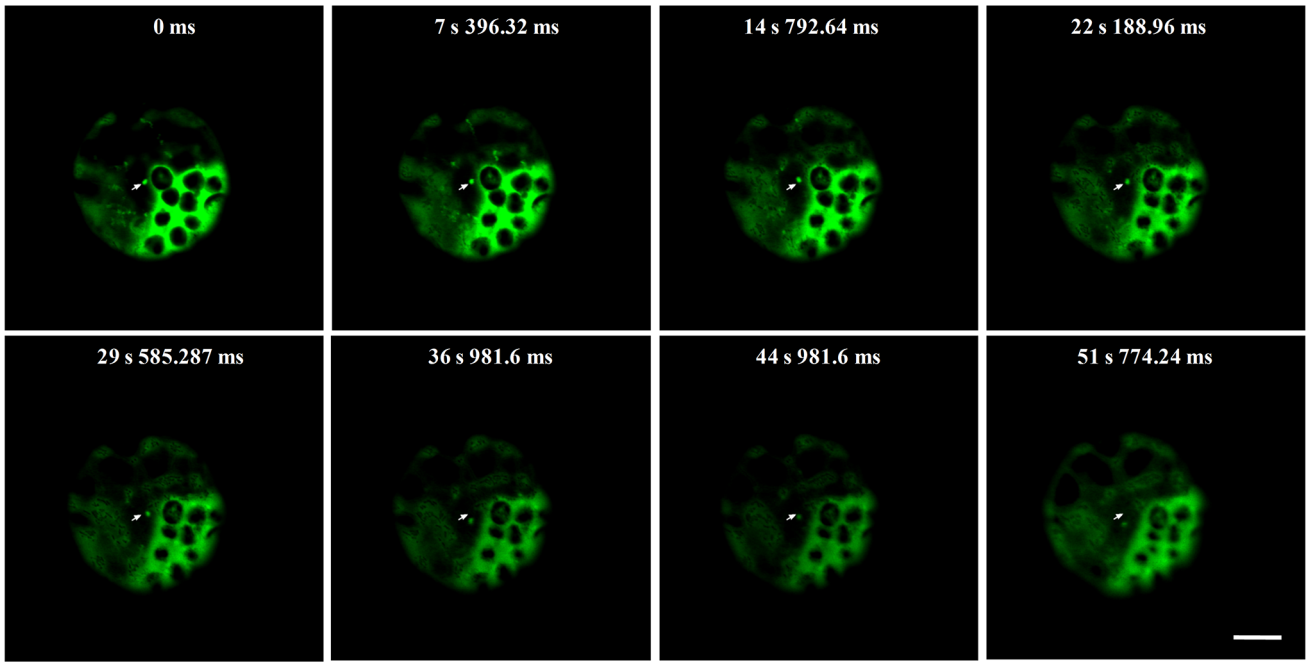

Fig. 4 The VpSTS29-containing bodies moved randomly in the cytoplasm. A time-lapse experiment was carried out to record the movement of VpSTS29-GFP-positive bodies in the cytoplasm. The time-lapse images were taken every 7 s. The STS29-containing bodies moved to different locations from one another. Scale bars = 10 µm. Images are extracted from Supplementary Movie S1

bodies marked by white arrows). We also observed that the less-intense fluorescence of VpSTS29-GFP in transgenic protoplasts connected physically with the oil bodies via tubular structures (Fig. 5a). However, most of the Nile red-stained oil bodies showed VpSTS29-GFP-negative patterns (Fig. 5b).

To confirm the localisation of VpSTS29-GFP in oil bodies stained with Nile red, the oil body marker caleosin 3 (CLO3) (Shimada et al. 2014) was expressed in the *Arabidopsis* protoplasts (Fig. 5c). The protein, CLO3 is from *Arabidopsis* (AT2G33380) fused to the C-terminal region of mCherry tag. We found the GFP-tagged spherical fluorescence merged completely with that marked by mCherry-CLO3 and moved apparently randomly in the vacuole (Fig. 5d, bodies marked by white arrows). Furthermore, the co-localisation rate of VpSTS29-GFP and mCherry-CLO3 in the senescent leaves was approximately twice than that in the young leaves (Fig. 5e). These results suggest the VpSTS29-containing bodies are indeed the leaf oil bodies and the translation of VpSTS29 into these oil bodies is induced by senescence.

STS-containing oil bodies are transported into the vacuoles in senescent leaves of grapevine

To confirm the movement of STS-containing bodies in the vacuole (Fig. 5e), transmission electron microscopy (TEM) and immunofluorescence analysis using the anti-STS antibodies were carried out in grapevine. The leaves of grapevine were pre-treated in darkness for 4 days. The control was cultured under normal light conditions. Compared with the control (Fig. 6a), the cell internal structure was changed in the senescent leaves (Fig. 6b). We observed electron-dense material (Fig. 6c, white dotted ellipse) and oil-body-like organelles (Fig. 6d, e) wrapped in vesicle-like structures in the vacuole. The immunofluorescence analysis using anti-STS antibodies confirmed the STS-containing oil bodies were transported into the vacuole (Fig. 6f, white arrow). These changes suggest STS is transported into the vacuole in dark-induced senescent leaves.

The stability of stilbene synthase in STS-containing oil bodies and in the vacuole

We had already observed that VpSTS29-GFP was translocated to oil bodies in senescent leaves (Fig. 5). Therefore, we investigated the influence of over-expression of CLO3 on the stability level of VpSTS29 protein (Fig. 7a). The 150 µl of transgenic *Arabidopsis* protoplasts with transiently expressed mCherry-CLO3 were incubated as above. Along with the increase of mCherry-CLO3 plasmids, the amount of VpSTS29-GFP protein was nearly unchanged (Fig. 7a). In addition, free GFP was not detected.

Transferring plants from light to dark can stabilise the GFP fluorescence in the vacuoles by abolishing the light-dependent degradation of GFP protein (Tamura et al.

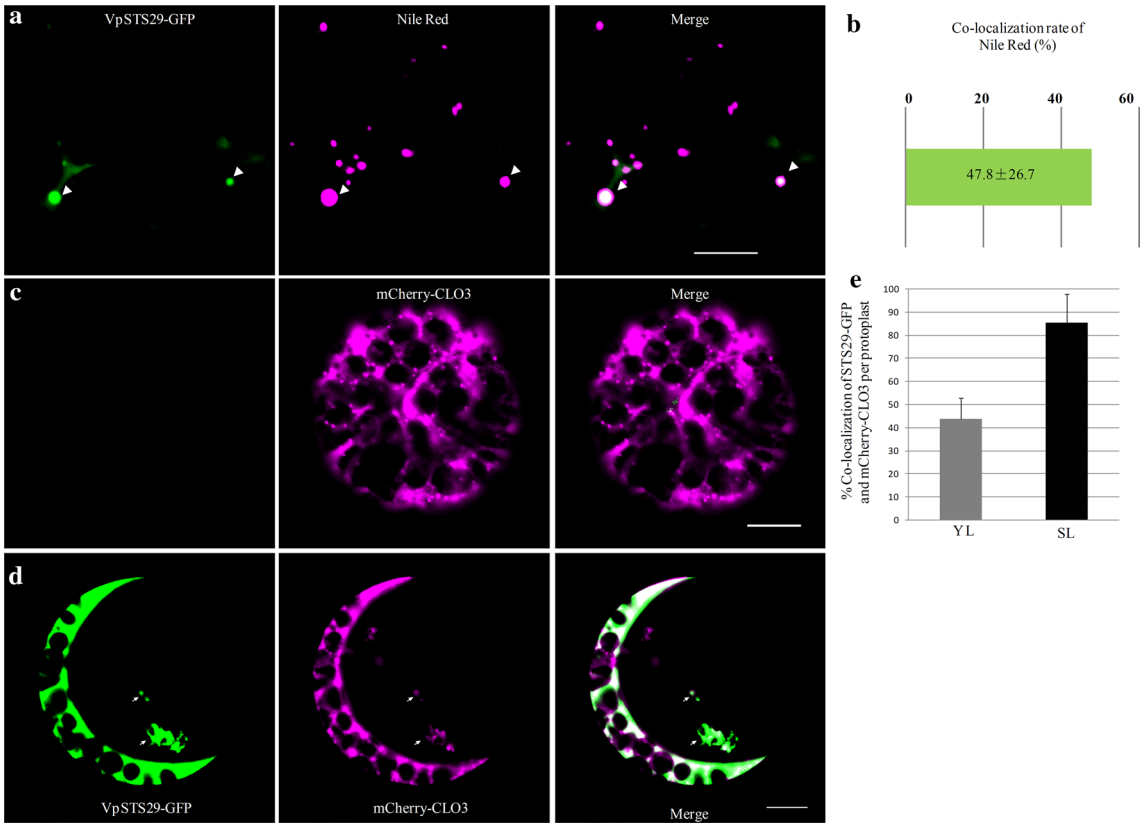

Fig. 5 VpSTS29-GFP was transported to the oil bodies. **a** Localisation of VpSTS29-GFP to the oil bodies stained with Nile red in *Arabidopsis* protoplasts. The VpSTS29-GFP-positive oil bodies are marked by white arrows. The connection between oil bodies was via a tubular structure. Scale bar = 10 µm. **b** Quantitative analysis of the co-localisation rate of oil bodies stained with Nile red and labelled with VpSTS29-GFP in five fluorescence images. A total of 80 oil bodies were examined. Data indicate average values ± standard deviation ($n = 5$). **c** The subcellular location of OB marker mCherry-CLO3. Scale bar = 10 µm. **d** The subcellular location of VpSTS29-GFP with mCherry-CLO3 in *Arabidopsis* protoplasts. Scale bar = 10 µm. The Nile red and mCherry tag show magenta. **e** Quantitative analysis of the co-localisation rate of VpSTS29-GFP and mCherry-CLO3 in protoplasts isolated from young and senescent leaves. A total of 33 oil bodies in 4 confocal images from young leaves and a total of 95 oil bodies in 5 confocal images from senescent leaves were counted. Error bars show standard deviation. *YL* young leaves, *SL* senescent leaves

2003). To determine the protein profile of the GFP-tagged VpSTS29 in the vacuole, 2-week-old transgenic *Arabidopsis* seedlings were treated in the dark for 3 days and then transferred to the light for another 12 h. As reported, the cleaved GFP protein can be used to monitor the breakdown of substrates within plant vacuoles by western blot (Klionsky et al. 2012). Total proteins were extracted at the times indicated and subjected to SDS-PAGE followed by immunoblot analysis with anti-GFP antibodies (Fig. 7b). The 70.5-kDa fusion protein consistent with VpSTS29-GFP was accumulated during the dark treatment. However, in the light, the level of VpSTS29-GFP decreased rapidly within 1 h but then increased again between 2 and 12 h. No bands consistent with free GFP (having a molecular mass of 27 kDa) were detected during the dark–light cycle. These results indicate the protein located in STS-containing oil bodies and in the vacuole is VpSTS29.

Constitutive overexpression of *VpSTS29* delays leaf senescence in *Arabidopsis*

We hypothesise that STS may function in plant growth. This is based on the expression and subcellular location profiles of this protein, on the metabolic products and on the phenotype in p*VpSTS29::VpSTS29*-expressed *Arabidopsis*. To test this, we generated transgenic *Arabidopsis* overexpressing *VpSTS29* under the control of the CaMV35S promoter (Fig. 8a). Compared with the controls, differences were apparent in 4-week-old plants, where inflorescences appeared 2 days later in the 4-week-old *VpSTS29*-OEs (Fig. 8b). In addition, in 6-week-old *VpSTS29*-OEs, the basal rosette leaves remained green. While in the controls, most were yellow (Fig. 8c). HPLC analysis showed that *trans*-piceid was significantly

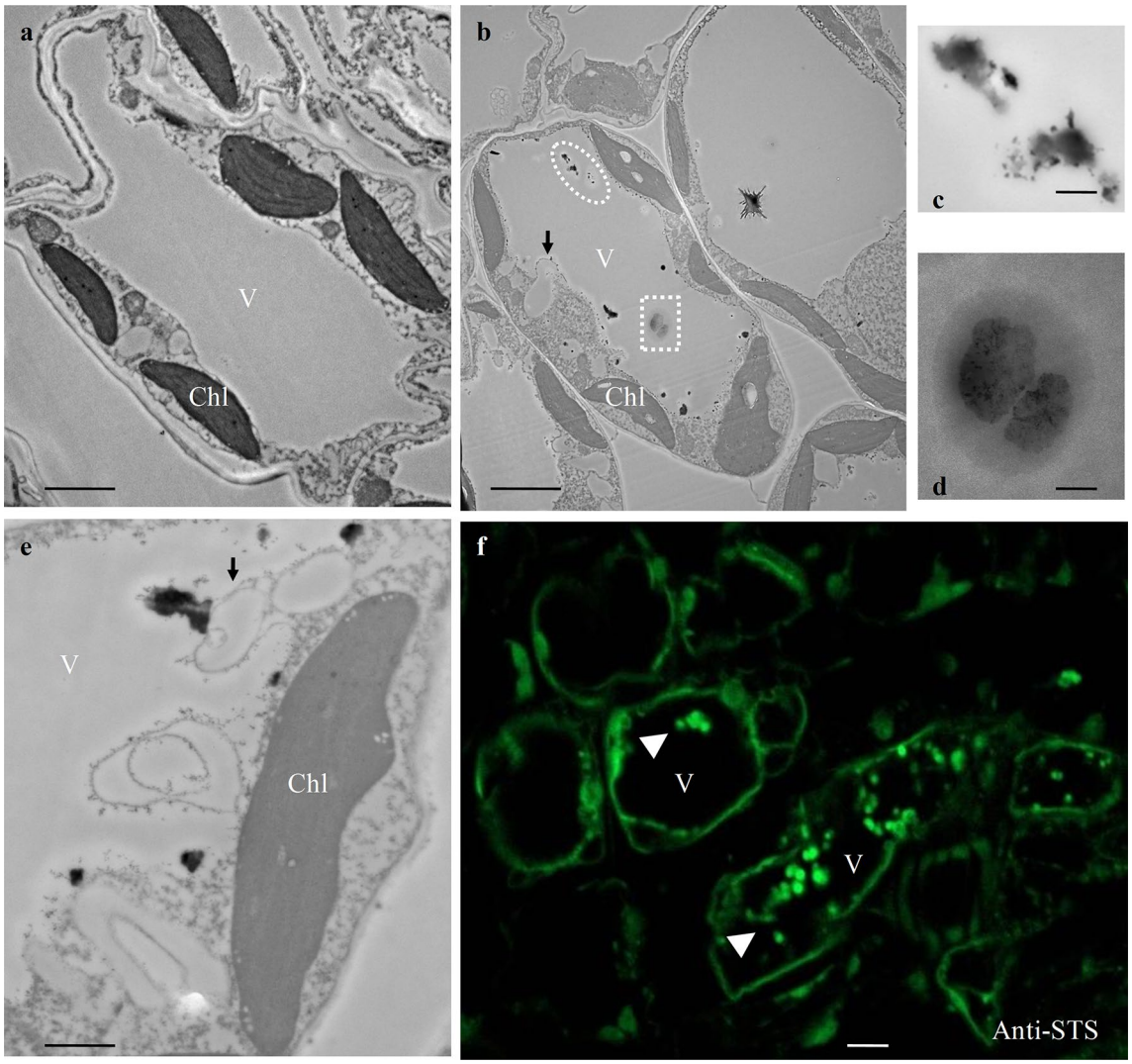

Fig. 6 The distribution of STS-containing bodies to the vacuole in grape. **a**–**e** Transmission electron-microscope (TEM) analysis of the change in the internal structure in grape leaves under a 4-day dark treatment. The leaves of the control (**a**) and the dark-induced transgenic grapes (**b**) were observed by TEM. The white-dotted ellipse indicates strongly electron-dense materials (**c**). White-dotted rectangles indicate oil-bodies-like structures (**d**). Black arrow indicates vesicle-like structures (**e**). *Chl* chloroplast, *V* vacuole. Scale bars = 2 µm. **f** The immunofluorescence assays in grape leaves under a 4-day dark treatment using anti-STS antibodies. *V* vacuole. White arrows, STS-containing OBs. Scale bar = 10 µm

accumulated in the 5- and 6-week-old *VpSTS29*-OEs (Fig. 8d). Furthermore, two senescence parameters (Oh et al. 1997), chlorophyll contents and photochemical efficiency of PSII, were used to determine the function of STS in delaying leaf senescence. Consistent with the above, chlorophyll contents were higher in *VpSTS29*-OEs than in the controls (Fig. 8e). In addition, the *VpSTS29*-OE plants retained relatively high levels of photochemical efficiency in the 6th week after sowing, while the photochemical efficiency of PSII was greatly reduced in the control (Fig. 8f). These results indicate that leaf senescence was delayed in *VpSTS29*-OEs.

Discussion

Stilbene compounds are derived from the stilbene synthesis pathway (Dixon 2001). Resveratrol has attracted much interest over many years, serving as the precursor of the stilbenes, as a phytoalexin and as a cancer chemo-preventive agent (Baur and Sinclair 2006; Shen et al. 2009; Sirerol et al. 2016). STS is the key enzyme catalysing the production of trihydroxystilbene resveratrol. Here, we have considered the expression profiles of STS and its metabolic products during plant growth and development, with a special focus on the cytosolic oil bodies containing STS and a possible role of VpSTS29 over-expression in leaf senescence.

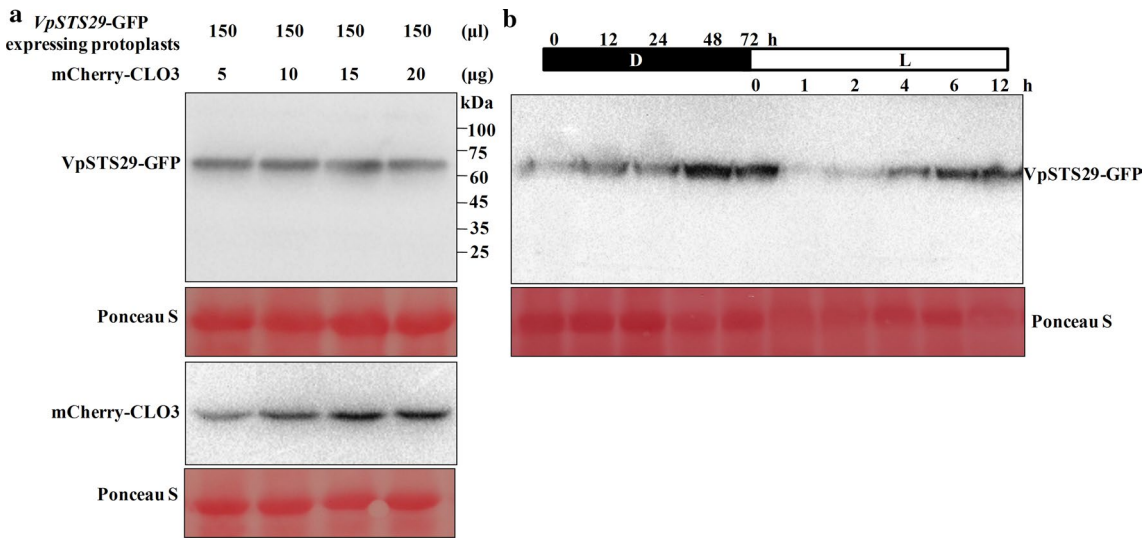

Fig. 7 The protein profiles of VpSTS29-GFP in transgenic *Arabidopsis*. **a** The influence of CLO3 on the protein profile of VpSTS29-GFP. 150 µl of p*VpSTS29*::*VpSTS29-GFP* expressing protoplasts were transformed with different contents of plasmid mCherry-CLO3. Samples were collected after protoplasts had been cultured for 24 h. Samples (20 µg) of total protein from protoplasts were subjected to western blot with a specific antibody against green fluorescent protein (GFP) and mCherry, respectively. **b** The protein profile of VpSTS29-GFP in transgenic *Arabidopsis* during a dark–light cycle. The 2-week-old p*VpSTS29*::*VpSTS29*-GFP transgenic plants were transferred to dark conditions (D) for 12, 24, 48 or 72 h, and then incubated under light conditions (*L*) for 1, 2, 4, 6 or 12 h. Samples (20 µg) of total protein from seedlings were subjected to western blot with a specific antibody against GFP

A global transcriptomic atlas of grapevine (*V. vinifera*) has been generated and this offers a powerful tool for gene-functional analysis (Fasoli et al. 2012). Genome-wide expression profiles of the grapevine *STS* genes show almost all members of *STSs* are strongly accumulated in senescing grape leaves and berries under withering conditions (Vannozzi et al. 2012). In this study, we report the expression of STS and also that stilbenes are accumulated in age-dependent and in dark-induced senescent leaves of grapevine (Fig. 1). Six standards (*trans*-resveratrol, *cis*-resveratrol, *trans*-piceid, *cis*-piceid, pterostilbene, and ε-viniferin) were used for HPLC analysis (Supplemental Fig. S2). According to the retention time, *trans*-resveratrol, *trans*-piceid, and *cis*-piceid were identified in different leaf positions and *trans*-piceid, and *cis*-piceid were identified in leaves after darkness treatment in the present investigation (Fig. 1b, e). Furthermore, the expressions of *MYB13*/*MYB15* and STS protein were closely correlated with the accumulation of stilbene compounds in grape leaves (Supplemental Fig. S1). It has previously been demonstrated that *MYB15* regulates the expression of *STS*s and induces the accumulation of *trans*-piceid in grapevine hairy roots (Höll et al. 2013). Therefore, the senescence process could activate the expression of *MYB15* and *STS*s to synthesise the stilbene compounds.

Since the first example of its purification and characterisation was reported by Schöppner and Kindl (1984), the genetic transformation of STS genes from stilbene-producing plants has been attempted a number of times. These attempts have been both intra-specific and inter-specific. Heterologous expression of the *STS* gene family members has been well-documented in model plants (Yu et al. 2006; Giovinazzo and Degara 2005; Hain et al. 1993), crops (Baek et al. 2012; Leckband 1998; Richter et al. 2006; Serazetdinova et al. 2005) and also in fruit trees (Cheng et al. 2016; Hanhineva et al. 2009; Kobayashi et al. 2000; Rühmann et al. 2006; Zhu et al. 2005). The transgenic plants produced displayed enhanced tolerance to various stresses and accompanied by the accumulation of stilbene compounds. In our work, ectopic expression of *VpSTS29* in *Arabidopsis* under its own promoter also induced the accumulation of VpSTS29 protein and *trans*-piceid, especially in senescing leaves (Fig. 2c, d). When over-expressed in *Arabidopsis* under CaMV35S promoter, the *VpSTS29*-OE plants exhibited delayed leaf senescence with high levels of chlorophyll content and of PSII photochemical efficiency (Fig. 8). Hence, STS and its product play a crucial role in the process of plant senescence.

The subcellular localisations of the enzymes involved in biosynthesis of phenylpropanoids have been explored over many years. Evidence shows the cytosolic side of the ER is responsible for the synthesis of lignin, isoflavonoid, flavonol, proanthocyanidin and anthocyanin (Winkel 2004; Chanoca et al. 2015; Gomez et al. 2011; Hrazdina et al. 1987). However, the site of resveratrol biosynthesis in grape has still to be determined. Using the transgenic *Arabidopsis* ectopically expressing *VpSTS29*-GFP, we have shown that VpSTS29

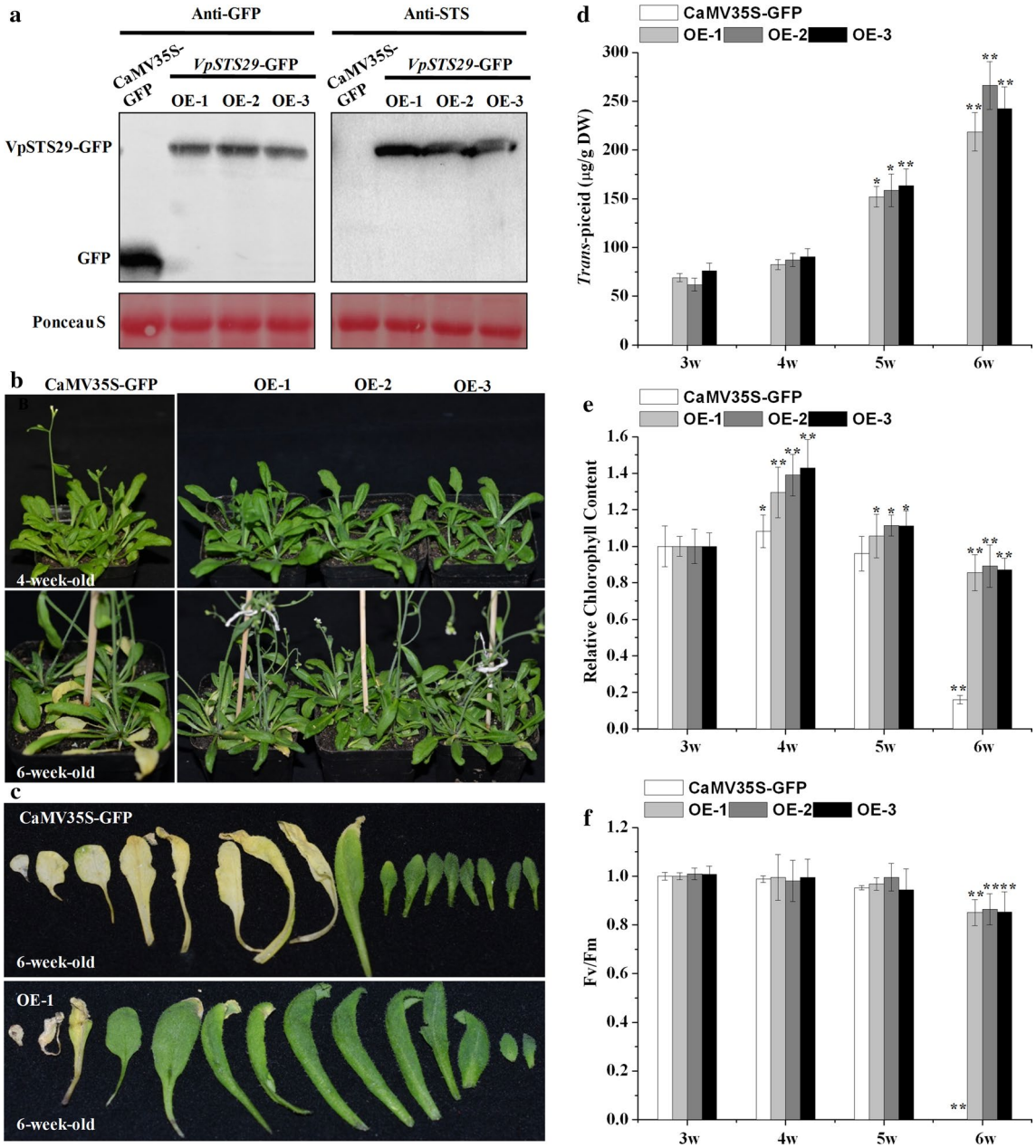

Fig. 8 Over-expression of VpSTS29 delays leaf senescence. **a** The identification of CaMV35S::*VpSTS29-GFP* expressing transgenic *Arabidopsis* by the immunoblotting assay with a specific antibody against GFP and grape STS, respectively. **b** The representative phenotypes of 4- and 6-week-old CaMV35S-GFP and *VpSTS29*-OE transgenic plants. **c** Representative phenotypes of leaves from the rosettes of 6-week-old CaMV35S-GFP and *VpSTS29*-OE transgenic plants during age-dependent senescence. **d** HPLC analysis of stilbene compounds in *VpSTS29*-OE transgenic plants at the weeks after sowing indicated. Significant difference was assessed by the least significant difference (LSD) test (**$P < 0.01$ and *$P < 0.05$). Error bars show SD from three independent experiments. Chlorophyll contents (**e**) and photochemical efficiency (F_v/F_m) of PSII (**f**) of CaMV35S-GFP and *VpSTS29*-OE leaves at the indicated weeks after sowing. Three biological replicates were carried out. The significant difference test was assessed by the least significant difference (LSD) test (**$P < 0.01$ and *$P < 0.05$). Error bars show SD from three independent experiments

is located in the cytoplasm or ER-like structures in protoplasts from young leaves (Fig. 3a). The subcellular location of STS was in accordance with that of CHS (Hrazdina et al. 1987; David and Brenda 2001). We note that both of these share the highly homologous amino acid sequence of stilbene-producing plants (Tropf et al. 1994). Meanwhile, in senescent protoplasts VpSTS29 was also distributed in unknown bodies (Fig. 3b). The localisations of enzymes involved in the phenylpropanoid pathway to the as-yet-unknown structures have still to be properly characterised.

However, some enzymes are also found in as-yet-unknown compartments or microsomes (Winkel 2004). The proper identification of these structures should help us to understand how plant cells synthesise and accumulate these phenylpropanoid products (Winkel 2004).

In this study, we observed the movement of VpSTS29-containing bodies in the cytoplasm by time-lapse imaging (Fig. 4). Nile red staining and co-localisation with organelle marker caleosin 3 (CLO3) confirmed these VpSTS29-containing bodies were lipid droplets/oil bodies (Fig. 5a and d), which are the lipid storage organelles of most eukaryotic cells (Martin and Parton 2006; Farese and Walther 2009). The inter-organelle communication of STS may be related to the potential roles of these oil bodies in phytoalexin synthesis. In *Arabidopsis,* CLO3 and a-dioxygenase (a-DOX1) were co-localised to the oil body membrane and produced phytoalexin in response to fungal infection (Shimada et al. 2014). The relationship of STS-containing bodies with pathogen infections in grape requires further exploration.

Moreover, the localisation of VpSTS29 into oil bodies was induced in senescent protoplasts (Fig. 5d, e). The increased rates of co-localisation may be in accordance with increases in the numbers of oil bodies in the cotyledons of wild-type *Arabidopsis thaliana* grown in darkness (Leivar et al. 2009). These are densely packed with oil bodies (Leivar et al. 2009). All these findings show that the formation of these bodies occurs at particular developmental stages of the plant's life cycle.

The oil bodies found in most eukaryotic cells are dynamic organelles (Martin and Parton 2006), that play important roles in the storage of neutral lipids, lipid metabolism, transient protein-storage and responses to pathogens (Welte 2015; Shimada and Hara-Nishimura 2015). Here, we show that the STS-containing bodies (oil bodies) were present in the cytoplasm or the vacuole both in transgenic *Arabidopsis* (Fig. 5c, d) and in grapevine (Fig. 6f). No bands of free GFP or GFP variants were detected in CLO3-VpSTS29 expressing protoplasts or *VpSTS29* expressing seedlings during dark–light cycles (Fig. 7). The fluorescence located in the cytoplasm, in oil bodies and in vacuoles was the VpSTS29-GFP fusion protein. The behaviour of STS trafficking to the vacuole may be related with the accumulation of stilbenes. The autofluorescence observations of stilbenes at the cell level in grapes have been used to monitor their distribution (Poutaraud et al. 2007; Donnez et al. 2011). The blue stilbene autofluorescence has been clearly observed in the vacuoles of epidermal cells and spongy parenchyma, as well as in the guard-cell walls in grapevine leaves under *Plasmopara viticola* infection (Bellow et al. 2012). In other stilbene-producing plants, such as the Norway spruce, stilbenes have been localised in the phloem parenchyma cells (Li et al. 2012), where other phenolic materials are also accumulated in the vacuoles (Krokene 2015). On the other hand, the dynamic inter-organelle communication of secondary metabolites is well understood, such as with flavonoid (Jian 2015; Zhao and Dixon 2010). The pigment anthocyanin is transported from the cytosolic side of the ER to the vacuole and stored in anthocyanin vacuolar inclusions (AVIs) by the microautophagy mechanism (Chanoca et al. 2015). This suggests a link with the transport of STS and the accumulation of resveratrol after its synthesis in stilbene-producing plants. Our results imply that the behaviour of STS-containing oil bodies trafficking to the vacuole is not for degradation but for stilbene storage. Therefore, in future research, a comparative analysis of the transport mechanisms of STS and its products should offer useful insights into their functions in response to environmental stress.

In conclusion, we have addressed the expression patterns of STS both in grape and in transgenic *Arabidopsis* by molecular, genetic and microscopic fluorescence approaches during age-dependent and dark-induced senescence. Our observations highlight the behaviours of STS, giving new insights into how the synthesis and transport of stilbenes. The relationship between STS trafficking to the vacuole and the storage of resveratrol, will be further explored in future work. This information will be crucial beyond its role in understanding stilbene accumulation, for developing better understandings of protection against pathogen attack and of environmental stress responses. All these will help researchers to exploit the STS gene resource from Chinese wild *Vitis* species for improving and breeding new grapevine cultivars both to improve berry quality and also to enhance stress defence (Jeandet et al. 2017).

Author contribution statement YW and FM designed the research. FM and LW carried out the experiments. FM analysed the results. FM wrote the manuscript. YW revised the manuscript. All authors read and approved the manuscript.

Acknowledgements This work was supported by the Grants from the National Science Foundation of China (Grant No. 31672129). The authors specifically thank Dr Alexander (Sandy) Lang from RESCRIPT Co. (New Zealand) for useful comments and language editing which have greatly improved the manuscript.

References

Achnine L, Blancaflor EB, Rasmussen S, Dixon RA (2004) Colocalization of L-phenylalanine ammonia-lyase and cinnamate 4-hydroxylase for metabolic channeling in phenylpropanoid biosynthesis. Plant Cell 16(11):3098–3109

Baek SH, Shin WC, Ryu HS, Lee DW, Moon E, Seo CS, Hwang E, Lee HS, Ahn MH, Jeon Y (2012) Creation of resveratrol-enriched rice for the treatment of metabolic syndrome and related diseases. PLoS ONE 8(3):e57930

Bassard JE, Werck-Reichhart D (2012) Protein–protein and protein–membrane associations in the lignin pathway. Plant Cell 24(11):4465–4482

Baur JA, Sinclair DA (2006) Therapeutic potential of resveratrol: the in vivo evidence. Nat Rev Drug Discov 5(6):493–506

Bellow S, Latouche G, Brown SC, Poutaraud A, Cerovic ZG (2012) In vivo localization at the cellular level of stilbene fluorescence induced by *Plasmopara viticola* in grapevine leaves. J Exp Bot 63(10):3697–3707

Bernales S, McDonald KL, Walter P (2006) Autophagy counterbalances endoplasmic reticulum expansion during the unfolded protein response. PLoS Biol 4(12):e423

Chanoca A, Kovinich N, Burkel B, Stecha S, Bohorquez-Restrepo A, Ueda T, Eliceiri KW, Grotewold E, Otegui MS (2015) Anthocyanin vacuolar inclusions form by a microautophagy mechanism. Plant Cell 27(9):2545–2559

Cheng S, Xie X, Xu Y, Zhang C, Wang X, Zhang J, Wang Y (2016) Genetic transformation of a fruit-specific, highly expressed stilbene synthase gene from Chinese wild *Vitis quinquangularis*. Planta 243(4):1–13

Clough SJ, Bent AF (1998) Floral dip: a simplified method for *Agrobacterium*-mediated transformation of *Arabidopsis thaliana*. Plant J 16(6):735–743

David S, Brenda WS (2001) Localization of flavonoid enzymes in *Arabidopsis* roots. Plant J 27(27):37–48

Dercks W, Creasy LL (1989) The significance of stilbene phytoalexins in the *Plasmopara viticola*-grapevine interaction. Physiol Mol Plant Pathol 13(4):351–371

Dixon RA (2001) Natural products and plant disease resistance. Nature 411(6839):843–847

Donnez D, Kim KH, Antoine S, Conreux A, Luca VD, Jeandet P, Clément C, Courot E (2011) Bioproduction of resveratrol and viniferins by an elicited grapevine cell culture in a 2L stirred bioreactor. Process Biochem 46(5):1056–1062

Dubrovina A, Kiselev K (2017) Regulation of stilbene biosynthesis in plants. Planta 246:597–623

Ehlting J, Büttner D, Wang Q, Douglas CJ, Somssich IE, Kombrink E (1999) Three 4-coumarate: coenzyme A ligases in *Arabidopsis thaliana* represent two evolutionarily divergent classes in angiosperms. Plant J 19(1):9–20

Farese RV, Walther TC (2009) Lipid droplets finally get a little R-E-S-P-E-C-T. Cell 139(5):855–860

Fasoli M, Dal Santo S, Zenoni S, Tornielli GB, Farina L, Zamboni A, Porceddu A, Venturini L, Bicego M, Murino V (2012) The grapevine expression atlas reveals a deep transcriptome shift driving the entire plant into a maturation program. Plant Cell Online 24(9):3489–3505

Ferrer JL, Jez JM, Bowman ME, Dixon RA, Noel JP (1999) Structure of chalcone synthase and the molecular basis of plant polyketide biosynthesis. Nat Struct Biol 6(8):775–784

Fornara V, Onelli E, Sparvoli F, Rossoni M, Aina R, Marino G, Citterio S (2008) Localization of stilbene synthase in *Vitis vinifera* L. during berry development. Protoplasma 233(1–2):83–93

Fritz K, Klaus H (1975) Enzymic synthesis of an aromatic ring from acetate units. Partial purification and some properties of flavanone synthase of cell-suspension cultures of *Petroselinum hortense*. Eur J Biochem 56(1):205–213

Giovinazzo G, Degara L (2005) Antioxidant metabolite profiles in tomato fruit constitutively expressing the grapevine stilbene synthase gene. Plant Biotechnol J 3(1):57–69

Gomez C, Conejero G, Torregrosa L, Cheynier V, Terrier N, Ageorges A (2011) In vivo grapevine anthocyanin transport involves vesicle-mediated trafficking and the contribution of anthoMATE transporters and GST. Plant J 67(6):960–970

Greenspan P, Mayer EP, Fowler SD (1985) Nile red: a selective fluorescent stain for intracellular lipid droplets. J Cell Biol 100(100):965–973

Hain R, Reif H, Krause E, Langebartels R, Kindl H, Vornam B, Wiese W, Schmelzer E, Schreier PH, Stöcker RH (1993) Disease resistance results from foreign phytoalexin expression in a novel plant. Nature 361(6408):153–156

Hammerbacher A, Ralph SG, Bohlmann J, Fenning TM, Gershenzon J, Schmidt A (2011) Biosynthesis of the major tetrahydroxystilbenes in spruce, astringin and isorhapontin, proceeds via resveratrol and is enhanced by fungal infection. Plant Physiol 157(2):876–890

Hanhineva K, Kokko H, Siljanen H, Rogachev I, Aharoni A, Kctrenlampi SO (2009) Stilbene synthase gene transfer caused alterations in the phenylpropanoid metabolism of transgenic strawberry (*Fragariaxananassa*). J Exp Bot 60(7):2093–2106

Herman EM (2008) Endoplasmic reticulum bodies: solving the insoluble. Curr Opin Plant Biol 11(6):672–679

Höll J, Vannozzi A, Czemmel S, D'Onofrio C, Walker AR, Rausch T, Lucchin M, Boss PK, Dry IB, Bogs J (2013) The R2R3-MYB transcription factors MYB14 and MYB15 regulate stilbene biosynthesis in *Vitis vinifera*. Plant Cell 25(10):4135–4149

Hrazdina G, Zobel AM, Hoch HC (1987) Biochemical, immunological, and immunocytochemical evidence for the association of chalcone synthase with endoplasmic reticulum membranes. Proc Natl Acad Sci USA 84(24):8966–8970

Huang L, Zhang S, Singer SD, Yin X, Yang J, Wang Y, Wang X (2016) Expression of the grape *VqSTS21* gene in *Arabidopsis* confers resistance to osmotic stress and biotrophic pathogens but not *Botrytis cinerea*. Front Plant Sci 7:1379

Jeandet P, Courot E, Clément C, Ricord S, Crouzet J, Aziz A, Cordelier S (2017) Molecular engineering of phytoalexins in plants: benefits and limitations for food and agriculture. J Agric Food Chem 65(13):2643–2644

Jian Z (2015) Flavonoid transport mechanisms: how to go, and with whom. Trends Plant Sci 20(9):576–585

Jiao Y, Xu W, Dong D, Wang Y, Nick P (2016) A stilbene synthase allele from a Chinese wild grapevine confers resistance to powdery mildew by recruiting salicylic acid signalling for efficient defence. J Exp Bot 67(19):5841–5856

Jørgensen K, Rasmussen AV, Morant M, Nielsen AH, Bjarnholt N, Zagrobelny M, Bak S, Møller BL (2005) Metabolon formation and metabolic channeling in the biosynthesis of plant natural products. Curr Opin Plant Biol 8(3):280–291

Jung E, Jensen RA (1986) Chloroplasts of higher plants synthesize L-phenylalanine via L-arogenate. Proc Natl Acad Sci USA 83(19):7231–7235

Kambiranda D, Katam R, Basha SM, Siebert S (2014) iTRAQ-based quantitative proteomics of developing and ripening muscadine grape berry. J Proteome Res 13(2):555–569

Klionsky DJ, Abdalla FC, Abeliovich H, Abraham RT, Acevedo-Arozena A, Adeli K, Agholme L, Agnello M, Agostinis P, Aguirre-Ghiso JA (2012) Guidelines for the use and interpretation of assays for monitoring autophagy. Autophagy 8(4):445–544

Kobayashi S, Ding CK, Nakamura Y, Nakajima I, Matsumoto R (2000) Kiwifruits (*Actinidia deliciosa*) transformed with a *Vitis* stilbene synthase gene produce piceid (resveratrol-glucoside). Plant Cell Rep 19(9):904–910

Krokene P (2015) Conifer defense and resistance to bark beetles. Bark beetles: biology and ecology of native and invasive species. Elsevier, Oxford, pp 177–207

Langcake P, Pryce RJ (1976) The production of resveratrol by *Vitis vinifera* and other members of the Vitaceae as a response to infection or injury. Physiol Plant Pathol 9(1):77–86

Leckband GH (1998) Transformation and expression of a stilbene synthase gene of *Vitis vinifera* L. in barley and wheat for increased fungal resistance. Theor Appl Genetics 96(8):1004–1012

Leivar P, Tepperman JM, Monte E, Calderon RH, Liu TL, Quail PH (2009) Definition of early transcriptional circuitry involved in light-induced reversal of PIF-imposed repression of photomorphogenesis in young Arabidopsis seedlings. Plant Cell 21(11):3535–3553

Li SH, Nagy NE, Hammerbacher A, Krokene P, Niu XM, Gershenzon J, Schneider B (2012) Localization of phenolics in phloem parenchyma cells of Norway spruce (*Picea abies*). ChemBioChem 13(18):2707–2713

Li Z, Peng J, Wen X, Guo H (2013) Ethylene-insensitive3 is a senescence-associated gene that accelerates age-dependent leaf senescence by directly repressing miR164 transcription in Arabidopsis. Plant Cell 25(9):3311–3328

Li Y, Im Kim J, Pysh L, Chapple C (2015) Four isoforms of Arabidopsis 4-coumarate: CoA ligase have overlapping yet distinct roles in phenylpropanoid metabolism. Plant Physiol 169(4):2409–2421

Martin S, Parton RG (2006) Lipid droplets: a unified view of a dynamic organelle. Nat Rev Mol Cell Biol 7(5):373–378

Oh SA, Park JH, Lee GI, Paek KH, Park SK, Nam HG (1997) Identification of three genetic loci controlling leaf senescence in *Arabidopsis thaliana*. Plant J 12(3):527–535

Pan QH, Wang L, Li JM (2009) Amounts and subcellular localization of stilbene synthase in response of grape berries to UV irradiation. Plant Sci 176(3):360–366

Parage C, Tavares R, Réty S, Baltenweckguyot R, Poutaraud A, Renault L, Heintz D, Lugan R, Marais GA, Aubourg S (2012) Structural, functional, and evolutionary analysis of the unusually large stilbene synthase gene family in grapevine. Plant Physiol 160(3):1407–1419

Poutaraud A, Latouche G, Martins S, Meyer S, Merdinoglu D, Cerovic ZG (2007) Fast and local assessment of stilbene content in grapevine leaf by in vivo fluorometry. J Agric & Food Chem 55(13):4913

Richter A, Jacobsen HJ, Kathen AD, Lorenzo GD, Briviba K, Hain R, Ramsay G, Kiesecker H (2006) Transgenic peas (*Pisum sativum*) expressing polygalacturonase inhibiting protein from raspberry (*Rubus idaeus*) and stilbene synthase from grape (*Vitis vinifera*). Plant Cell Rep 25(11):1166–1173

Rippert P, Puyaubert J, Grisollet D, Derrier L, Matringe M (2009) Tyrosine and phenylalanine are synthesized within the plastids in Arabidopsis. Plant Physiol 149(3):1251–1260

Ro DK, Mah N, Ellis BE, Douglas CJ (2001) Functional characterization and subcellular localization of poplar (*Populus trichocarpa* × *Populus deltoides*) cinnamate 4-hydroxylase. Plant Physiol 126(1):317–329

Roy S (2000) Strategies for the minimisation of UV-induced damage. In: de Mora SJ, Demers S, Vernet M (eds) The effects of UV radiation in the marine environment. Cambridge University Press, Cambridge, pp 177–205

Rühmann S, Treutter D, Fritsche S, Briviba K, Szankowski I (2006) Piceid (resveratrol glucoside) synthesis in stilbene synthase transgenic apple fruit. J Agric Food Chem 54(13):4633–4640

Schöppner A, Kindl H (1984) Purification and properties of a stilbene synthase from induced cell suspension cultures of peanut. J Biol Chem 259(11):6806–6811

Serazetdinova L, Oldach KH, Lörz H (2005) Expression of transgenic stilbene synthases in wheat causes the accumulation of unknown stilbene derivatives with antifungal activity. J Plant Physiol 162(9):985–1002

Shen T, Wang X-N, Lou H-X (2009) Natural stilbenes: an overview. Nat Prod Rep 26(7):916–935

Shimada TL, Hara-Nishimura I (2015) Leaf oil bodies are subcellular factories producing antifungal oxylipins. Curr Opin Plant Biol 25:145–150

Shimada TL, Takano Y, Shimada T, Fujiwara M, Fukao Y, Mori M, Okazaki Y, Saito K, Sasaki R, Aoki K (2014) Leaf oil body functions as a subcellular factory for the production of a phytoalexin in *Arabidopsis*. Plant Physiol 164(1):105–118

Sirerol JA, Rodríguez ML, Mena S, Asensi MA, Estrela JM, Ortega AL (2016) Role of natural stilbenes in the prevention of cancer. Oxid Med Cell Longev 2016:3128951

Suzuki M, Nakabayashi R, Ogata Y, Sakurai N, Tokimatsu T, Goto S, Suzuki M, Jasinski M, Martinoia E, Otagaki S (2015) Multi omics in grape berry skin revealed specific induction of stilbene synthetic pathway by UV-C irradiation. Plant Physiol 168(1):47–59

Tamura K, Shimada T, Ono E, Tanaka Y, Nagatani A, S-i Higashi, Watanabe M, Nishimura M, Hara-Nishimura I (2003) Why green fluorescent fusion proteins have not been observed in the vacuoles of higher plants. Plant J 35(4):545–555

Thazar-Poulot N, Miquel M, Fobis-Loisy I, Gaude T (2015) Peroxisome extensions deliver the Arabidopsis SDP1 lipase to oil bodies. Proc Natl Acad Sci 112(13):4158–4163

Tropf S, Lanz T, Rensing SA, Schröder J, Schröder G (1994) Evidence that stilbene synthases have developed from chalcone synthases several times in the course of evolution. J Mol Evol 38(6):610–618

Vannozzi A, Dry IB, Fasoli M, Zenoni S, Lucchin M (2012) Genome-wide analysis of the grapevine stilbene synthase multigenic family: genomic organization and expression profiles upon biotic and abiotic stresses. BMC Plant Biol 12(1):1–22

Wang Y, Liu Y, He P, Chen J, Lamikanra O, Lu J (1995) Evaluation of foliar resistance to *Uncinula necator* in Chinese wild Vitis species. Vitis 34(3):159–164

Wang W, Tang K, Yang HR, Wen PF, Zhang P, Wang HL, Huang WD (2010) Distribution of resveratrol and stilbene synthase in young grape plants (*Vitis vinifera* L. cv. Cabernet Sauvignon) and the effect of UV-C on its accumulation. Plant Physiol Biochem 48(2):142–152

Weaver LM, Amasino RM (2001) Senescence is induced in individually darkened Arabidopsis leaves, but inhibited in whole darkened plants. Plant Physiol 127(3):876–886

Welte M (2015) Expanding roles for lipid droplets. Curr Biol 25(11):R470–R481

Winkel BS (2004) Metabolic channeling in plants. Annu Rev Plant Biol 55(4):85–107

Xu W, Yu Y, Ding J, Hua Z, Wang Y (2010) Characterization of a novel stilbene synthase promoter involved in pathogen- and stress-inducible expression from Chinese wild *Vitis pseudoreticulata*. Planta 231(2):475–487

Xu W, Yu Y, Zhou Q, Ding J, Dai L, Xie X, Xu Y, Zhang C, Wang Y (2011) Expression pattern, genomic structure, and promoter analysis of the gene encoding stilbene synthase from Chinese wild *Vitis pseudoreticulata*. J Exp Bot 62(8):2745

Xu W, Li R, Zhang N, Ma F, Jiao Y, Wang Z (2014) Transcriptome profiling of *Vitis amurensis*, an extremely cold-tolerant Chinese wild *Vitis* species, reveals candidate genes and events that potentially connected to cold stress. Plant Mol Biol 86(4):527–541

Yin X, Singer SD, Qiao H, Liu Y, Jiao C, Wang H, Li Z, Fei Z, Wang Y, Fan C (2016) Insights into the mechanisms underlying ultraviolet-C induced resveratrol metabolism in grapevine (V. amurensis Rupr.) cv. "Tonghua-3". Front. Plant Sci 7:503

Yoo SD, Cho YH, Sheen J (2007) Arabidopsis mesophyll protoplasts: a versatile cell system for transient gene expression analysis. Nat Protoc 2(7):1565–1572

Yu CKY, Lam CNW, Springob K, Schmidt J, Chu IK, Lo C (2006) Constitutive accumulation of *cis*-piceid in transgenic arabidopsis overexpressing a sorghum stilbene synthase gene. Plant Cell Physiol 47(7):1017

Zhao J, Dixon RA (2010) The 'ins' and 'outs' of flavonoid transport. Trends Plant Sci 15(2):72–80

Zhu YJ, Agbayani R, Jackson MC, Tang CS, Moore PH (2005) Expression of the grapevine stilbene synthase gene *VST1* in papaya provides increased resistance against diseases caused by *Phytophthora palmivora*. Planta 220(2):241–250